

ORIGINAL ARTICLE

Metabolic Dysregulation of the Lysophospholipid/Autotaxin Axis in the Chromosome 9p21 Gene SNP rs10757274


Sven W. Meckelmann¹, PhD*; Jade I. Hawksworth, MSc*; Daniel White¹, PhD; Robert Andrews¹, PhD; Patricia Rodrigues¹

Correspondence to: Valerie O'Donnell, PhD, Systems Immunity Research Institute, Cardiff University, School of Medicine, Heath Park, Cardiff, CF14 4XN, United Kingdom. Email o-donnellvb@cardiff.ac.uk

*Dr Meckelmann and J.I. Hawksworth contributed equally to this work.

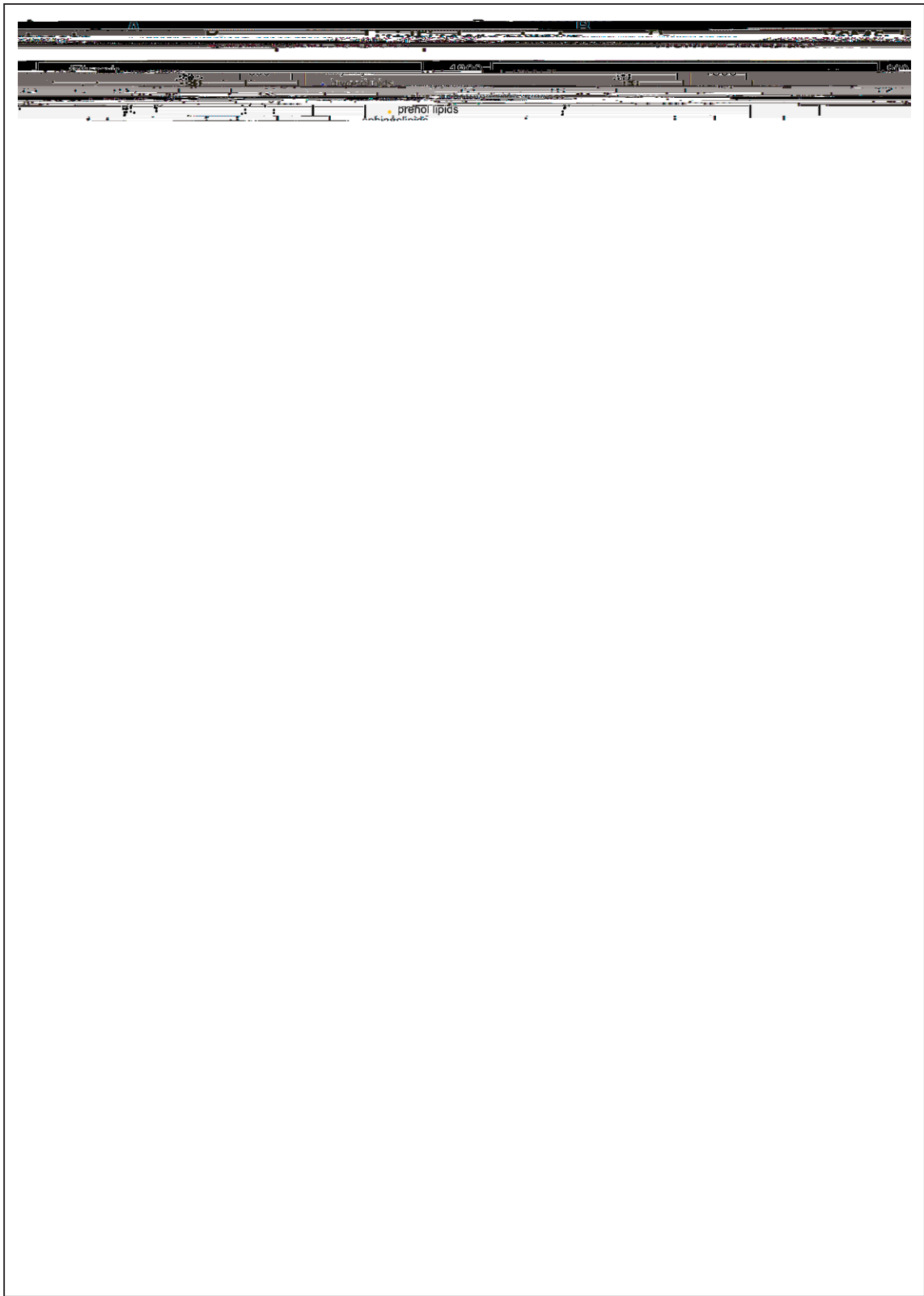
The Data Supplement is available at <https://www.ahajournals.org/doi/suppl/10.1161/CIRCGEN.119.002806>.

For Sources of Funding and Disclosures, see page 163.

© 2020 The Authors.  is published on behalf of the American Heart Association, Inc., by Wolters Kluwer Health, Inc. This is an open access article under the terms of the [Creative Commons Attribution](https://creativecommons.org/licenses/by/4.0/) License, which permits use, distribution, and reproduction in any medium, provided that the original work is properly cited.

 is available at www.ahajournals.org/journal/circgen

The association of altered plasma lipids with coro



Those most affected by genotype were glycerophospholipids and unknowns (Figure 1C through 1J, Table 1). Following F value adjustment the number of significantly different lipids was 17, with 7 putatively identified as lysoPC ions and adducts (Tabs I and II in the [Data Supplement](#)). An additional group of 8 had p values close to significance at 0.05 to 0.08. All were reduced in GG plasma. As this method is used as for hypothesis generation only, we next validated our results using gold-standard quantitative targeted methods.



The same plasmas were analyzed using a targeted fully quantitative assay for 15 lysoPLs (lysophospholipids). Of these several lysoPCs significantly decreased, with both lysoPC and lysoPEs all trending towards lower levels in GG (Figure IVA in the [Data Supplement](#)). This was replicated using new samples from NPHSII (n=47: AA, 49: GG; Figure IV in the). [This was](#)

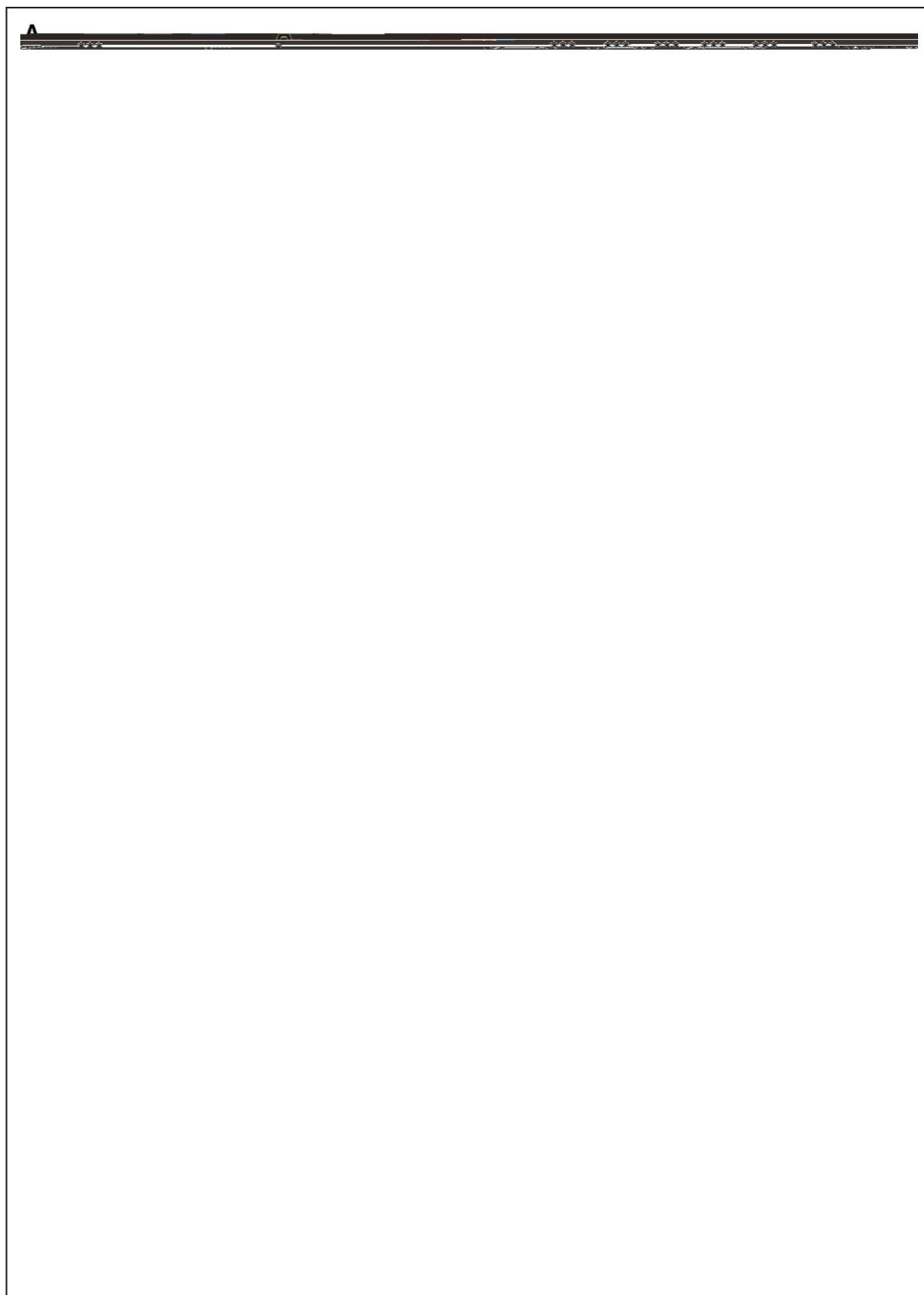


Figure 2. LysoPLs (Lysophospholipids) are significantly reduced in rs10757274 GG but not in subjects with unrelated SNPs. **A**, Several LPCs are lower in GG samples than AA controls, and LPEs trend towards lower levels. LysoPLs were determined using LC/MS/MS as described in Methods (n=88 AA and 81 GG). Tukey box plot, * <0.05, ** <0.01, *** <0.005, 2-tailed, unpaired Student test (black) and Mann-Whitney (red). **B**, Plasma lysoPL are not altered by other risk SNPs. Plasma from the NPHSII (Northwick Park Heart Study II) cohort containing several risk (up or down) SNPs were analyzed using LipidFinder, and m/z values corresponding to lysoPL extracted and

was seen in GG, suggesting a decoupling of ATX from metabolizing lysoPL to lysoPA. Comparing the slopes for AA versus GG revealed significant differences based on genotype ($p = 0.0157$). This further underscores the dysregulation of the lysoPL metabolic pathway in the GG group and suggests that non-ATX pathways may mediate lysoPL to lysoPA conversion. Last, the relative ratios of all lysoPL and lysoPA molecular species were unchanged in the GG versus AA groups (Figure 3L). Thus, while metabolism of lysoPL/lysoPA by ATX is altered, there was no influence of genotype on molecular composition overall. Notably, ATX preferentially metabolizes unsaturated lysoPCs.¹⁸ Overall, despite the correlations only showing associations, when taken with our observations that plasma from GG subjects has significantly less ATX protein and that all lysoPC molecular species are similarly affected, our data strongly evidence that there is less involvement of ATX in metabolizing these lipids in GG plasmas.

Next, a Pearson correlation analysis looking at relationships between individual lipids and ATX was next undertaken using Cytoscape. For thresholds, the classification system of Schober was used.¹⁹ Here, we see that there are moderate ($r = 0.40$ – 0.69 , green) or strong ($r = 0.70$ – 1.00 , gray) correlations between lipids of the same class, while there are weak ($r = 0.10$ – 0.39 , red) correlations between different lipid classes (Figure 4A). Importantly, the key difference in the data set is that the weak correlations between classes are positive for the AA group, while they are negative for the GG group (Figure 4A). Overall, this indicates that these lipids behave similarly within AA subjects. In contrast, in GG plasma, while lipid classes still positively correlate within their groups (eg, lysoPCs correlate strongly with each other), the links between lysoPL and lysoPA are lost. Instead correlations were weakly negative between lysoPE and lysoPA (Figure 4A). As in Figure 4, ATX weakly positively correlates with lysoPA in the AA group but instead with lysoPL in the GG group. This analysis reinforces our findings of altered metabolism for lysoPL/lysoPA but here at the level of individual lipid species.

shRNA downregulation of the proximal ANRIL transcripts EU741058 and DQ485454 in HEK-293 cells at 48 and 96 hours.¹² ANRIL plicudpresRion of the p () TJ 0.068 Tw10 -1.201 TD ((EU7410and)Tfi (lism Genctfi



Chr9p21 risk SNPs are believed to act via altering expression of ANRIL, which regulates cell proliferation/senescence in vitro.^{2,4,5} To examine for a functional link with lysoPL/lysoPA metabolism, we analyzed the effect of

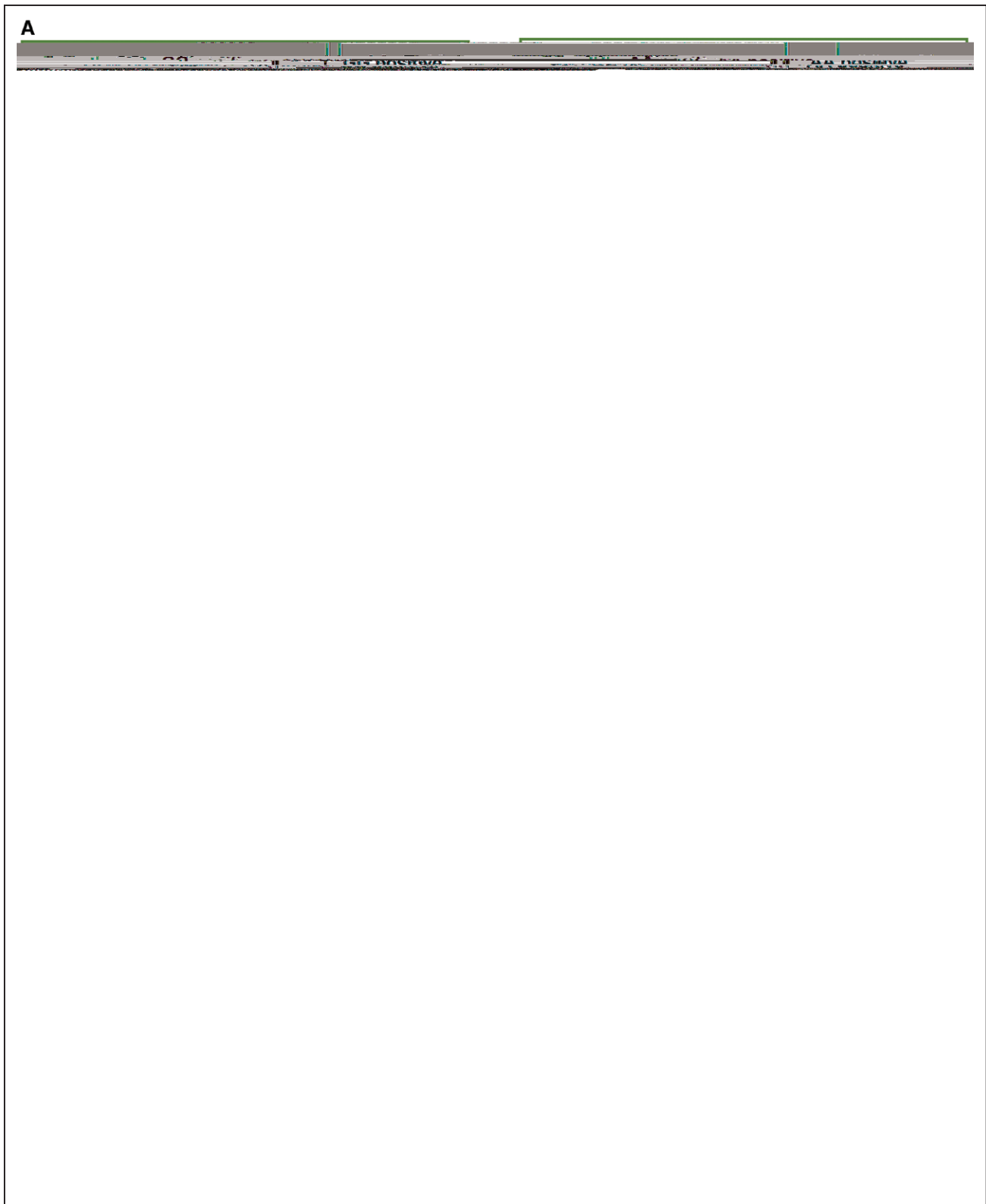


Figure 4. Cytoscape analysis of lipids reveals divergent metabolism in GG vs AA, while ANRIL knockdown is associated with significant changes to lysoPL (lysophospholipids)/lysoPA (lysophosphatidic acid)-metabolizing genes.

A, Cytoscape reveals strong links within related families, but a positive-negative switch for lysoPL-lysoPA correlations between AA-GG plasmas. Pearson correlation networks were generated for the AA and GG validation samples (n=47 AA and 49 GG), using lipid concentrations. Nodes are colored by lipid sub-category and represent individual molecular species, and edges represent the correlation. Edges detail the Pearson correlation coefficients between nodes (lipids), where the width of the edge denotes value. Additionally, edges are colored by value: red (=0.10–0.39); green (=0.40–0.69); gray (=0.70–1.00). ()

Figure 4 Continued. C and D. Significant changes in lipid regulatory gene expression are observed with ANRIL knockdown in cell culture. Affymetrix array data generated in Congrains et al⁵ was analyzed using GO as described in Methods. Volcano plot showing differential gene expression of all genes on the Affymetrix HuGene1.0 v1, chip. LysoPL/lysoPA regulating genes that alter in line with decreased levels of the lipids in GG plasma are labeled. The horizontal dashed line shows where adj. p value < 0.05 (Benjamini-Hochberg correction) where points (genes) above this line are significantly differentially expressed. LysoPL-regulating genes that alter in line with decreased levels of the lipids are labeled in black. Genes in red are annotated to the GO term detailed in the plot title. Data are plotted in R using ggplot2. **B**, Forty-eight hour shRNA knockdown. **C**, Ninety-six hour shRNA knockdown.

significantly different between risk haplotypes (RRWT) and other lines, and where removal of the risk locus in RR led to partial or complete rescue: β and β (Figure 5A, Figure VI in the [Data Supplement](#)). Of these, β were regulated in line with reduced lysoPC/lysoPA.

Multivariate analysis using principal component analysis for expression of these 14 genes shows clear separation of VSMC lines containing the RRWT from controls (NNWT) in PC-1 (Figure 5B). When the risk locus was deleted, the resulting RRKO cell lines instead clustered closer to NNWT and NNKO in PC-1 (Figure 5B). This analysis indicates that expression of several lysoPL metabolizing genes is different in risk haplotype cells but reverts closer to NN on removal of the 9p21 locus.

Next, correlations of genes that metabolize lysoPLs with ANRIL isoforms (exons 6–7 and 18–19) were performed. Deletion of the Chr9p21 locus in the KO VSMC lines starts around exon 9 and runs downstream to the end of the coronary artery disease region.¹³ Analysis of ANRIL was performed by qPCR detection of ANRIL isoforms containing exons 6 and 7 (present in long and short isoforms) and exons 18 to 19 (in long isoforms only). The analysis showed a significant increase of isoforms containing exons 6 and 7 in RRWT cells, compared with NNWT cells (Figure VII in the [Data Supplement](#)), as previously described.¹³ ANRIL expression was minimal in NNWT, with levels comparable to a residual expression of ANRIL detected in both KO lines, possibly due to transcription of truncated transcripts. ANRIL analysis performed using detection of exons 18 and 19 showed no significant differences between RRWT and NNWT cells. No transcript expression was detected in KO lines as expected because the deletion encompasses the last 10 exons of the ANRIL gene. These analyses confirmed that ANRIL short isoforms containing exons 6 and 7 but not 18 and 19 are upregulated in RRWT VSMCs. To evaluate possible correlations between lysoPLs-related genes and ANRIL expression, all samples were used for ANRIL (exons 6–7) analysis, while for correlations with ANRIL (exons 18–19), only WT (RR and NN) were tested. Circular ANRIL isoforms have not been detected in these cells.

ANRIL (Exons 6–7)

Several genes correlated significantly, either in a positive or a negative direction with these ANRIL isoforms (Figure VIII in the [Data Supplement](#)). RRWT samples (in red) clustered

together as groups, separated from all other samples, which were seen to express phospholipid (PL) metabolism genes similarly. This was somewhat expected because these PL metabolism genes were differently expressed in RRWT versus RRKO, NNWT, NNKO, as shown for ANRIL (6–7) expression (Figure 5B, Figure VII in the [Data Supplement](#)). However, the significant Pearson correlations between ANRIL (exons 6–7), and the individual genes show a direct association between this form of these ANRIL isoforms and some lysoPL genes.

ANRIL (Exons 18–19)

Here, correlations were tested using RRWT or NNWT clones separately and then compared. Five genes were identified where a significant negative correlation between ANRIL (18–19) and lysoPL gene expression was seen (β , β , and β) in the RR clones. In contrast, correlations in NN samples were weaker and not significant (Figure IX in the [Data Supplement](#)). This suggests an impact of ANRIL (18–19) isoforms on gene expression, that is absent/reduced in NN. One NN clone displayed higher levels of ANRIL (18–19) compared with others, and as an outlier had a large impact on the correlation, reducing statistical power.



ANRIL displays sponge activity towards miRNAs.²⁰ To examine whether this could mechanistically link ANRIL with lysoPL gene expression, we undertook an in-silico analysis using 2 databases (including one that is experimentally validated: TarBase v8 (http://carolina.imis.athena-innovation.gr/diana_tools/web/index.php?r=tarbasev8%2Findex) and TargetScan (http://www.targetscan.org/vert_72/)). We searched whether miRNAs known to be inhibited by ANRIL interact with PL-metabolizing genes that are altered in HEK or VSMC data sets. Here, the expected outcome is that target genes should be regulated in the same direction as ANRIL. Some hits were found, including 2 that were conserved across both data sets. In the HEK data, the miRNAs that interact with downregulated genes were miR-186-3p, miR-34a-3p (β) and miR-122-5p, miR-34a-5p (β). In the VSMC data set, where ANRIL (exons 6–7) is significantly upregulated in RR, we focused on genes that were elevated in RR and reduced

when the locus was deleted. Here, we found miR-34a-5p (▲) and miR-122-5p (▲). These hits were all from the experimentally validated database (Tarbase)

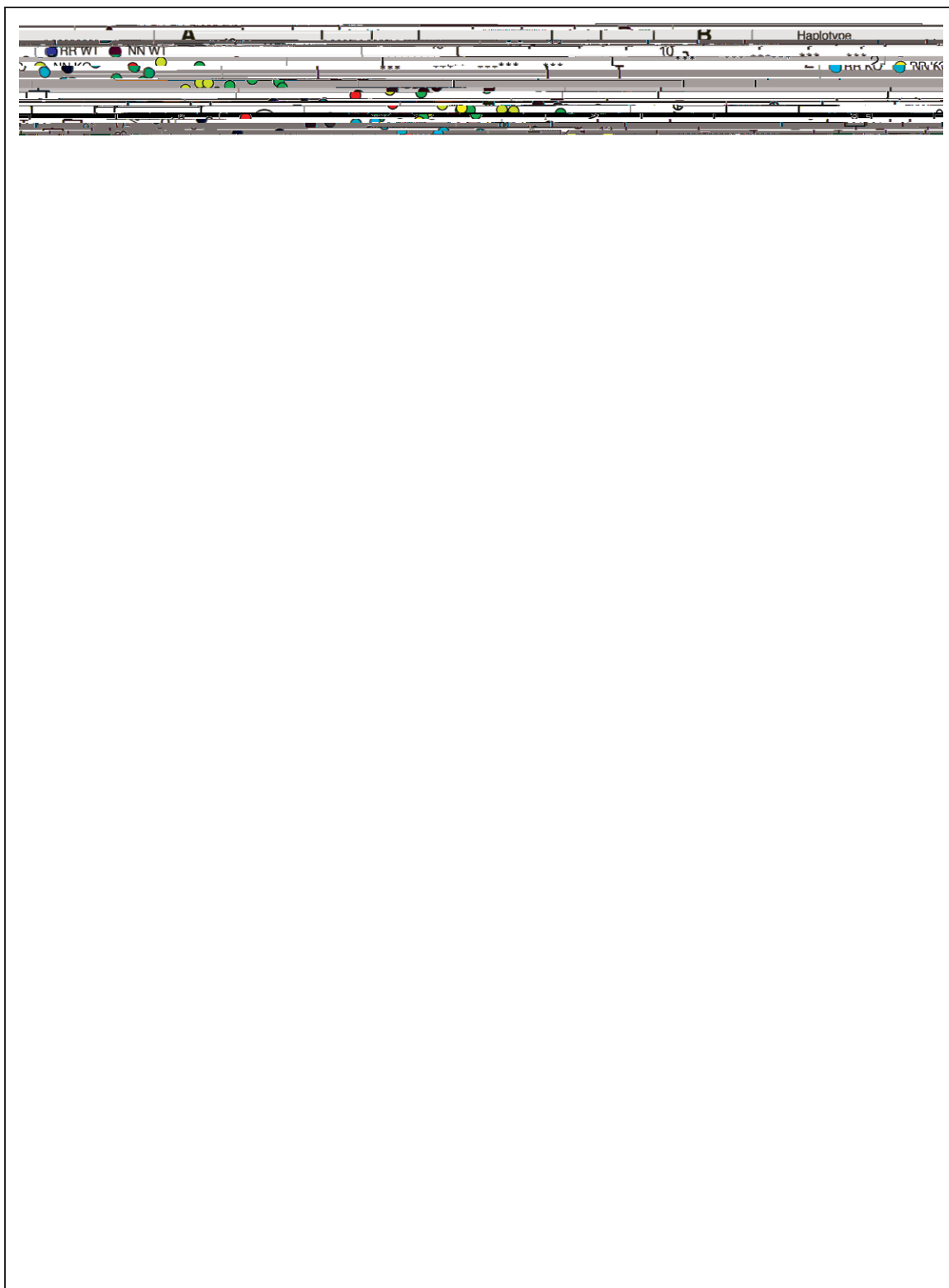


Figure 5. VSMCs from risk haplotypes show differential gene expression of lysoPL (lysophospholipid) metabolizing genes that are rescued by deletion of the Chr9p21 locus.

A, PCA shows that the presence of risk haplotypes is associated with differential gene expression of lysoPL genes. Induced pluripotent stem cells from peripheral monocytes were obtained and differentiated as described in Materials in the [Data Supplement](#). RNAseq data were clustered using lysoPL metabolizing genes by PCA in R. Nonrisk haplotype (NNWT), risk haplotype (RRWT) and their genome edited counterparts (NNKO and RRRKO) are shown. **B**, Example data sets for ACSL3 and DGKA, showing that removing the risk locus reverts gene expression back to levels in nonrisk individuals. * <

metabolic alterations to the lysoPL/lysoPA/ATX axis in human plasma (Figures 1 through 4). This revealed a gen-

In line with this, [\[redacted\]](#) expression negatively correlated with ANRIL (exons 18–19) in VSMC from the risk group, suggesting an association between this gene and a risk form of ANRIL (Figure IX in the [Data Supplement](#)). Also,

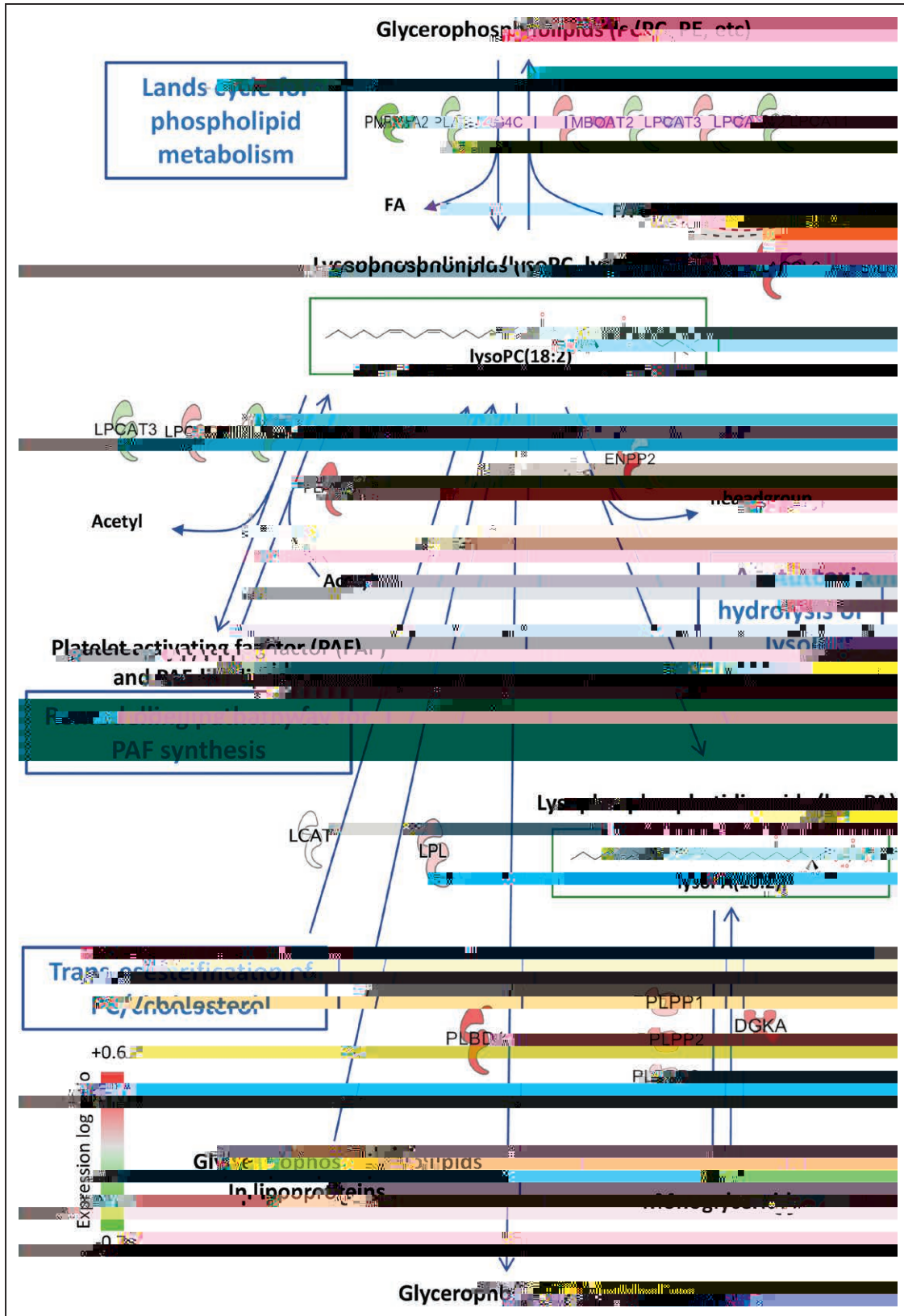


Figure 6. Metabolic pathway showing lysoPL (lysophospholipids)/lysoPA (lysophosphatidic acid) regulatory genes that are significantly altered by ANRIL knockdown in HEK cells. Genes that metabolize these lipids are shown. Full data on their transcriptional regulation is provided in Table 3, Tab VII in the Data Supplement. LCAT was not significantly regulated but is shown for completeness.

- increasing the number of tests. *PLoS One*. 2009;10:209. doi: 10.1186/1471-2105-10-209
16. Aoki J, Taira A, Takanezawa Y, Kishi Y, Hama K, Kishimoto T, Mizuno K, Saku K, Taguchi R, Arai H. Serum lysophosphatidic acid is produced through diverse phospholipase pathways. *J Biol Chem*. 2002;277:48737–48744. doi: 10.1074/jbc.M206812200
 17. Wuensch KL. Comparing correlation coefficients, slopes and intercepts. 2007. Available at: <http://core.ecu.edu/psyc/wuenschk/docs30/CompareCorrCoeff.pdf>. Accessed June 3, 2020.
 18. Kurano M, Suzuki A, Inoue A, Tokuhara Y, Kano K, Matsumoto H, Igarashi K, Ohkawa R, Nakamura K, Dohi T, et al. Possible involvement of minor lysophospholipids in the increase in plasma lysophosphatidic acid in acute coronary syndrome. *PLoS One*. 2015;35:463–470. doi: 10.1161/ATVBAHA.114.304748
 19. Schober P, Boer C, Schwartze LA. Correlation coefficients: appropriate use and interpretation. *PLoS One*. 2018;126:1763–1768. doi: 10.1213/ANE.0000000000002864
 20. Kong Y, Hsieh CH, Alonso LC. ANRIL: a lncRNA at the CDKN2A/B locus with roles in cancer and metabolic disease. *PLoS One*. 2018;9:405. doi: 10.3389/fendo.2018.00405
 21. Alshehry ZH, Mundra PA, Barlow CK, Mellett NA, Wong G, McConville MJ, Simes J, Tonkin AM, Sullivan DR, Barnes EH, et al. Plasma lipidomic profiles improve on traditional risk factors for the prediction of cardiovascular events in type 2 diabetes mellitus. *Circulation*. 2016;134:1637–1650. doi: 10.1161/CIRCULATIONAHA.116.023233
 22. Cheng JM, Suoniemi M, Kardys I, Vihervaara T, de Boer SP, Akkerhuis KM, Sysi-Aho M, Ekroos K, Garcia-Garcia HM, Oemrawsingh RM, et al. Plasma concentrations of molecular lipid species in relation to coronary plaque characteristics and cardiovascular outcome: results of the ATHEROREMO-IVUS study. *Atherosclerosis*. 2015;243:560–566. doi: 10.1016/j.atherosclerosis.2015.10.022
 23. Havulinna AS, Sysi-Aho M, Hilvo M, Kauhanen D, Hurme R, Ekroos K, Salomaa V, Laaksonen R. Circulating ceramides predict cardiovascular outcomes in the population-based FINRISK 2002 cohort. *PLoS One*. 2016;36:2424–2430. doi: 10.1161/ATVBAHA.116.307497
 24. Hinterwirth H, Stegemann C, Mayr M. Lipidomics: quest for molecular lipid biomarkers in cardiovascular disease. *PLoS One*. 2014;7:941–954. doi: 10.1161/CIRCGENETICS.114.000550
 25. Holčápek M, Červená B, Cífková E, Lisa M, Chagovets V, Vostálová J, Bancíková M, Galuszka J, Hill M. Lipidomic analysis of plasma, erythrocytes and lipoprotein fractions of cardiovascular disease patients using UHPLC/MS, MALDI-MS and multivariate data analysis. *J Chromatogr B*. 2015;990:52–63. doi: 10.1016/j.jchromb.2015.03.010
 26. Jové M, Naudí A, Portero-Otin M, Cabré R, Rovira-Llopis S, Bañuls C, Rocha M, Hernández-Mijares A, Victor VM, Pamplona R. Plasma lipidomics discloses metabolic syndrome with a specific HDL phenotype. *PLoS One*. 2014;28:5163–5171. doi: 10.1096/fj.14-253187
 27. Laaksonen R. Identifying new risk markers and potential targets for coronary artery disease: the value of the lipidome and metabolome. *PLoS One*. 2016;30:19–32. doi: 10.1007/s10557-016-6651-8
 28. Lu J, Chen B, Chen T, Guo S, Xue X, Chen Q, Zhao M, Xia L, Zhu Z, Zheng L, et al. Comprehensive metabolomics identified lipid peroxidation as a prominent feature in human plasma of patients with coronary heart diseases. *PLoS One*. 2017;12:899–907. doi: 10.1016/j.redox.2017.04.032
 29. Meikle PJ, Wong G, Barlow CK, Kingwell BA. Lipidomics: potential role in risk prediction and therapeutic monitoring for diabetes and cardiovascular disease. *PLoS One*. 2014;14:12–23. doi: 10.1016/j.pharmthera.2014.02.001
 30. Rankin NJ, Preiss D, Welsh P, Sattar N. Applying metabolomics to cardiovascular intervention studies and trials: past experiences and a roadmap. *PLoS One*. 2014;9:1–10. doi: 10.1371/journal.pone.0100000